

## Calibration of Soil Moisture for Large-Eddy Simulations over the FIFE Area

J. L. EASTMAN

*Graduate Degree Program in Ecology and Department of Atmospheric Science, Colorado State University, Fort Collins, Colorado*

R. A. PIELKE AND D. J. McDONALD

*Department of Atmospheric Science, Colorado State University, Fort Collins, Colorado*

(Manuscript received 8 March 1996, in final form 5 May 1997)

### ABSTRACT

A case day, 11 October 1987, was chosen for simulation using the Regional Atmospheric Modeling System (RAMS). The day was unique from other "golden" days of the First International Satellite Land Surface Climatology Project (ISLSCP) Field Experiment (FIFE) in that the surface wind speeds were light in terms of magnitude. Numerous datasets were used to initialize the meteorology, vegetation, canopy height, roughness length, topography, and soil properties.

The simulation was performed using the RAMS nested grid feature. First, the large-scale flow reproduced by RAMS was evaluated against the observations taken during FIFE and archived data available at the National Center for Atmospheric Research. Next, a large-eddy simulation (LES) was integrated for a 6-h period starting at 1500 UTC 11 October 1987. FIFE surface flux and surface thermodynamic and dynamic data were then used to evaluate the LES. It was found that LES fluxes were in poor spatial agreement with the observations, although domain-averaged values were in good agreement.

A technique for initializing the near-surface to surface soil moisture was then developed after finding a near-linear relationship between 6-h averaged latent heat and the initial model-gridded soil moisture obtained from an objective analysis of field data. The LES was performed again using the new soil moisture obtained from the relationship. The evaluation showed significant improvement in the model's ability to represent spatial heterogeneity of surface fluxes present on 11 October 1987.

### 1. Introduction

The complexity of surface characteristics contribute to difficulties in modeling surface energy and water budgets. Vegetation parameterizations in models require the specification of numerous values related to the vegetation. Leaf area index, vegetation fractional coverage, albedo, roughness length, canopy height, and characteristics of the plant root system all need to be initialized in order to carry out a simulation. Soil parameters, such as hydraulic conductivity, diffusivity, temperature profile, and moisture profile further add to the complexity, as well as the number of degrees of freedom employed in initializing a model.

The soil model used in the Regional Atmospheric Modeling System (RAMS) is directly dependent on curves derived by Clapp and Hornberger (1978). The thermal and hydrologic conductivities deduced from these curves for different soil types show standard de-

viations of an amplitude similar to the values at a given point on the curve. Given this degree of uncertainty, the concept of fixed values for a specified soil textural class lacks confidence over the large range of atmospheric and vegetative conditions over which it is applied.

The need for data to calibrate physically based parameterizations has been addressed in several large-scale experiments. The First International Satellite Land Surface Climatology Project (ISLSCP) Field Experiment (FIFE) is one such example. Others include the Boreal Ecosystem-Atmosphere Study (BOREAS) and the Hydrologic Atmospheric Pilot Experiment (HAPEX). The soil and biophysical datasets from FIFE are used in the following study to explore the sensitivity of the surface energy budget to the surface boundary conditions.

Analysis of the FIFE soil moisture dataset has been a focus of several papers (Peck et al. 1992; Ungar et al. 1992; Wang et al. 1992; Charpentier and Groffman 1992; Peck and Hope 1995; Chen and Brutsaert 1995). These studies investigate airborne and surface measurements made during many of the FIFE Intensive Field Campaigns (IFCs). It was noted in many of these studies that spatial variability was larger than expected. This makes the estimation of soil moisture needed to initialize a LES a difficult task. Not only does the soil

---

*Corresponding author address:* Dr. Roger A. Pielke, Department of Atmospheric Science, Colorado State University, Fort Collins, CO 80523.  
E-mail: eastman@stromboli.atmos.colostate.edu

TABLE 1. Average wind speeds for five “golden” days taken from the FIFE AMS data (averaged from 1500 through 2100 UTC using all available stations).

Date	$ \mathbf{u} $ (m s <sup>-1</sup> )
6 Jun 1987	9.3
11 Jul 1987	8.2
15 Aug 1987	8.0
11 Oct 1987	1.3
4 Aug 1989	6.7

moisture exhibit large spatial gradients, the composition of the soil displays similar variability. This degrades the validity of employing a single soil textural class used in many models and would point to a need to calibrate the physical characteristics of the soil on a site-by-site basis. In Wai and Smith (1998) it was demonstrated that results from several closure schemes achieved root-mean-square errors (RMSE) near the accuracy of the measurement devices when coefficients were calibrated for the FIFE dataset.

The variability of the surface parameters within the FIFE domain also leads to a large degree of variability in the flux measurements. For example, Chen and Brutsaert (1995) found a strong link between the spatial variability of soil moisture and the latent flux. Using analytic and numerical modeling, spatial variability of surface singularities has been shown to produce circulations that exhibit sensible and latent heat flux amplitudes that extend through the depth of the boundary layer and into the free troposphere (Avissar and Pielke 1989; Vidale et al. 1997). For LES the need to accurately depict the surface becomes imperative since these circulations can have a profound effect on the atmosphere depending on the large-scale flow. It has been demonstrated that, as the synoptic forcing becomes stronger, the mesoscale forcing may not be as important (Dalu et al. 1996).

During IFC1–4 of FIFE 1987, and IFC5 of FIFE 1989, there were five “golden” days selected. These days were given priority for processing by scientists. The “golden” days exhibit little, if any, cloud cover. Four of the five days also had strong winds prevalent. As mentioned in the previous paragraph, this tends to reduce the impact of smaller-scale variability and minimize the mesoscale contribution to the circulation. The average wind speeds for the golden days are shown in Table 1. Notice that on all days, except 11 October 1987, the wind speeds are in excess of 6.5 m s<sup>-1</sup>. This could lead to conclusions biased by strong winds in regard to variability within the FIFE area if only those days are used for the analysis of the effect of surface heterogeneity on the heat and moisture fluxes.

This study uses 11 October 1987 as a case day to validate RAMS over a variety of spatial and temporal scales. In addition, a method is devised to initialize near-surface soil moisture. The model is then integrated using

the new soil moisture fields and its performance re-evaluated.

## 2. Regional Atmospheric Modeling System

### a. Basic model setup

The RAMS model is a primitive equation prognostic model. For the simulations performed in this study, the model was integrated in three dimensions and contained four staggered Arakawa-type C grids (Fig. 1), each using nonhydrostatic, compressible equations on a terrain-following  $\sigma_z$  coordinate system (Gal-Chen and Somerville 1975; Mahrer and Pielke 1977). Leapfrog-in-time and second-order-in-space numerical schemes are used (Tripoli and Cotton 1982). Turbulent fluxes were calculated using a deformation  $K$  turbulence closure. The longwave and shortwave radiation scheme used is based on the Chen and Cotton (1983; 1987) procedure in which cloud attenuation effects are included. Nudging toward observed fields was used to suppress gravity wave reflections at the model top. Lateral boundaries were based on Klemp and Wilhelmson (1978a,b). For a complete model description, the reader is referred to Pielke et al. (1992) and Nicholls et al. (1995).

The horizontal grid spacing was 200, 800, 3200, and 12 800 m, with the coarse grid and 3200-m mesh employing 50 points in the horizontal directions. The 3200-m mesh used 38 points in each horizontal direction. The three coarse meshes contained 35 points in the vertical, with a constant vertical grid increment of 400 m. The finest mesh, which had 82 points in the horizontal directions, encompassing the entire FIFE domain, was also nested in the vertical, with a constant grid increment of 200 m for the lowest 14 points, and 400 m for eight more grid points, giving it a total vertical extent of 5.4 km.

### b. The vegetation and soil models

The vegetation model is based on the work of Avissar and Mahrer (1988). It is a one-layer vegetation model that calculates stomatal conductance, and latent and sensible heat fluxes at the top of the canopy. Surface characteristics of the vegetation used in the model are based on the the Biosphere–Atmosphere Transfer Scheme (BATS, Dickinson et al. 1986). There are a total of 18 BATS categories. Each class has its own characteristic values of albedo, roughness length, emissivity, leaf area index (LAI), fractional coverage, vegetation displacement height, and root depth.

In addition, a multilayer soil model, implementing the work of McCumber and Pielke (1981) and Tremback and Kessler (1985), is used to provide soil surface temperature, soil heat and moisture fluxes, and surface specific humidity to the vegetation model, as well as water availability in the various soil layers, depending on the length of the roots.

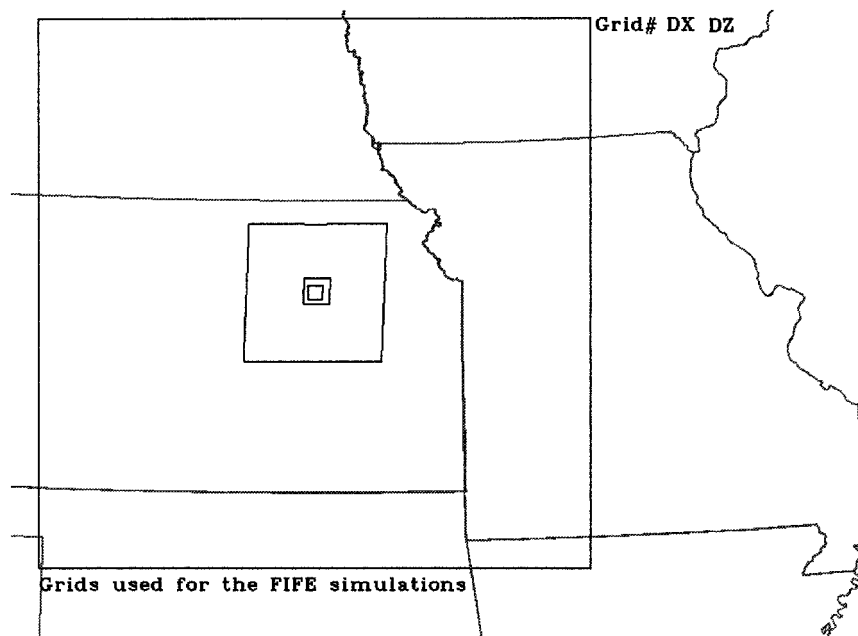


FIG. 1. Grid locations used for the FIFE simulations.

The soil moisture flux is a function of soil water potential gradient and soil hydraulic conductivity. The heat flux depends on soil thermal diffusivity, volumetric heat capacity, and soil density. The soil moisture and heat parameters can be defined for 12 classes of soil implemented in the RAMS soil model.

### 3. Initialization of the RAMS model

#### a. Meteorological initialization and nudging

There are several components of RAMS that allow the user to customize the model to simulate a particular situation. For the 10–11 October 1987 case, the meteorology for the initialization was objectively analyzed using  $2.5^\circ$  lat sized NMC, (now, known as the National Centers for Environmental Prediction) gridded data, surface observations, and rawinsondes. The objectively analyzed fields from  $12^\circ$  1200 UTC 10 October were used to initialize the momentum and thermodynamic fields in the model. Fields were also produced at 12-h intervals to nudge the model toward the observed fields, using a Newtonian relaxation technique. The relative strength of the nudging was strongest at the boundaries and dropped to  $1/16$  of the boundary value near the center of the domain. The nudging was only applied to the coarsest mesh for the simulations.

Measurements of incident shortwave radiation were also used to nudge the model-calculated incident shortwave radiation. An average value was obtained from stations that had contiguous measurements. The measurements were available in half-hour increments, and were themselves 30-min averages. The model-calculated incident shortwave was adjusted by taking the ratio

of the observed half-hour averaged shortwave to the model-calculated shortwave at the center of the domain, then applying this ratio to model shortwave calculations throughout the domain. The adjusted shortwave was found to be within 10% of the model calculations within a couple hours of solar noon; however, large zenith angle model calculations were found to be underpredicted.

#### b. Initialization of surface properties

The topography used for each grid was extracted from a dataset with 30-s horizontal spacing. Silhouette averaging was used for the topography, and feedback from the finer grids to the next coarser mesh allows for consistency between fine-grid averages and coarser mesh values.

For vegetation, the model uses 18 separate vegetation types defined according to the BATS classification scheme. In simulations that employed variable vegetation, the 30-s USGS vegetation dataset was selected to initialize each grid. The vegetation type in a particular grid cell is assigned the value of the most predominant vegetation class.

The vast dataset collected for FIFE provided the information needed to customize the vegetation characteristics, instead of using default values (Sellers et al. 1992). Included in the biological surveys is data describing LAI and canopy height. This was collected at various sites throughout the FIFE domain. This data was objectively analyzed, using a Barnes analysis, to the two finest grids employed in the simulations. Although the approximation is simple, it provides a better estimate

of LAI and canopy height than the default values in the RAMS model.

The LAI analyzed fields were also used to adjust the vegetation fractional coverage and roughness length. First, a ratio between the observed LAI and default model values was formed. This ratio was then applied to the vegetation fractional coverage maximum value. For example, instead of having 85% coverage wherever tall or short grass classes are used, values ranged from 58% to 85%. This coverage has a direct influence on the model-calculated heat fluxes. The roughness length was taken to be 13% of the canopy height value (Shuttleworth and Wallace 1985) obtained from the Barnes analysis. Again, the LAI ratio described above was applied to the roughness length. This corresponds to a reduction in roughness length as the vegetation coverage becomes sparse.

For the two coarsest meshes, the roughness length, LAI, and fractional coverage were set to the average value of the finest mesh. This corresponds to values of 0.034 m, 1.8, and 0.81, respectively.

In preliminary tests, it was found that there was a strong dependence of the Bowen ratio on the soil moisture and temperature profiles. The FIFE dataset again provided a valuable source of information. First, a soil class similar in composition to the soil survey results was constructed from an average of the survey results. Next, eight stations were used to objectively analyze the soil moisture to the RAMS soil model grid. The vertical grid structure was set to identical values used in the soil station data. The total depth used by the RAMS soil model was 1 m, with a reduction of vertical grid spacing from 0.2 m at the lowest level to 0.025 m for the top soil layer. The temperature profile used to initialize the RAMS soil model was an average of the stations. This soil data available was for 11 October 1987. Since the model was started at 1200 UTC 10 October, 2D simulations were conducted to back out the soil moisture and temperature profiles on the 10th. Thus, after 27 hours of integration on the coarse mesh, the temperature and soil moisture profiles matched the observed values within 3%. As with the vegetation parameters, the coarsest two grids used values obtained from the average of the FIFE domain.

#### 4. Case study: 10–11 October 1987

##### *a. Observations of 10–11 October 1987*

At 1200 UTC 10 October 1987, high pressure was centered over southeastern North Dakota. A cold front had passed through Kansas the previous day and had moved into Oklahoma. Conditions were generally overcast over the FIFE domain. Winds were from the northeast at 5–10 m s<sup>-1</sup> and increased in magnitude upward through the troposphere. Throughout the day the center of the high pressure was tracking south toward the northeast corner of Kansas. Mixing ratios remained relatively

constant throughout the next 24 hours, ranging from 2.4 to 2.8 g kg<sup>-1</sup>. Temperatures were 1° to 2°C and warmed up to about 11°C during the day. The soil was quite dry, about 40% of capacity.

At 1200 UTC 11 October 1987, the high pressure center was positioned over northeast Kansas. Associated with the system, temperatures were cooler and wind speeds had decreased to 1–2 m s<sup>-1</sup>. Winds were still generally from the north. Over the next 6 hours, the temperatures again reached 11°C, while the winds shifted, generally coming out of the southwest. The boundary layer was still quite dry, around 2.8 g kg<sup>-1</sup>, and changed little from 1200 to 1800 UTC. Skies were clear to partly cloudy over the FIFE domain. There were small amounts of precipitation recorded during the previous 24 hours (less than 2 mm). The scattered rain had stopped by 0400 UTC on the 11th. Soil moistures still hovered around 40% of capacity.

##### *b. Coarse grid simulation of 10–11 October 1987*

The model was integrated for a total of 33 hours starting at 1200 UTC 10 October 1987 and ending at 2100 UTC 11 October 1987. For the first 27 hours of integration, only the coarse mesh was used. The model data was averaged over 30-min intervals for several variables in order to facilitate comparison with the observations taken in the FIFE domain, which were also averaged over 30-min intervals. A bilinear interpolation scheme was used to obtain model values at the specific FIFE meteorological stations.

For the first 27 hours, the coarse grid interpolated values were compared to the observations for two sets of data: the archived surface observations from (NCAR) and the FIFE dataset. Pearson correlation coefficients and biases were computed for sensible and latent fluxes, evaporative flux fraction,  $U$  and  $V$  wind components, temperature, and mixing ratio. The wind components and temperature at the observational heights were obtained from the model using similarity theory since the lowest atmospheric model level above ground was at 200 m AGL. There were 40 stations used in NCAR data files, with each station evaluated at three separate times, 1200 UTC 10 October and 0000 and 1200 UTC 11 October. The results are displayed in Table 2.

The comparisons with the NCAR archived datasets show good agreement in terms of correlations, with all above 0.6. The model does indicate a cool bias for temperature. This is due to stronger nocturnal cooling than observed, possibly due to the lack of clouds which were not modeled in this simulation. In addition, the FIFE data is probably not valid for other portions of the domain where soil moisture and vegetation characteristics probably differ. The velocity fields are well represented by the model and there is little indication of a bias. The mixing ratio shows the lowest correlation, although it does indicate the model's ability to represent the moisture fields. The model dryness is likely due to the soil

TABLE 2. Correlation coefficients and bias for selected variables calculated from the indicated datasets for the coarse grid simulation. NCAR\* is the statistical comparison of model and observational data for the entire coarse grid domain for the period beginning 10 October at 1200 and ending at 2100 UTC 11 October. FIFE\* is the statistical comparison of model and FIFE observational data for the period beginning 10 October at 1200 UTC and ending on 11 October at 2100 UTC. FIFE\*\* is the statistical comparison of model and observational data for the period 1500–2100 UTC 11 October.

Variable	NCAR*		FIFE*		FIFE**					
	$r$	Bias	$r$	Bias	$r$	Bias	$E$	$E_{UB}$	$\sigma$	$\sigma_{obs}$
$H$ ( $W m^{-2}$ )	N/A	N/A	0.28	18.1	0.40	-4.90	99	99	101	75
$\lambda E$ ( $W m^{-2}$ )	N/A	N/A	0.06	29.4	0.17	-2.0	38	38	14	38
$\lambda E$										
$(H + \lambda E)$	N/A	N/A	0.03	-0.12	-0.002	-0.007	0.11	0.11	0.013	0.11
$u$ ( $m s^{-1}$ )	0.86	0.11	0.74	0.43	0.89	0.13	0.53	0.52	0.79	1.1
$v$ ( $m s^{-1}$ )	0.81	0.04	0.68	1.19	-0.12	-0.68	1.1	0.88	0.62	0.56
$\theta$ (K)	0.84	-1.09	0.84	-0.44	0.99	-0.27	0.50	0.42	2.5	2.4
$w$ ( $kg kg^{-1}$ )	0.66	-0.0013	0.47	0.0017	0.45	0.0006	0.0007	0.0005	0.00007	0.005

moisture and vegetation initialization, which was relatively dry and had low values of LAI. This would lead to lower evaporative and transpiration rates if other portions of the domain were wetter or had just received precipitation or had larger LAI.

The analysis was also carried out using the data collected for FIFE during this period. The FIFE data also included sensible and latent heat fluxes, which would also be included in the validation. Shown in Table 2 are the results for FIFE data taken over the entire 27-h period simulated, and a temporal subset taken from 1500 through 2100 UTC 11 October. The shorter time period corresponds to the times that the LES simulations were also performed. A total of 12 surface stations (AMS), and 19 surface flux stations (eddy correlation and Bowen ratio type) were used from the FIFE dataset.

The correlations for the 27-h period display good agreement, with  $r$  greater than 0.6 for velocity and temperature fields. The model's ability to predict the moisture field has degraded somewhat. Given the resolution of the coarse grid, roughly the size of the FIFE domain, the model still is doing a fair job of predicting the momentum and thermodynamic fields.

Table 2 also shows the correlations and bias for sensible and latent heat fluxes, as well as evaporative flux fraction, for the same 27-h time period. The data indicates poor agreement for the fluxes and their sum. This is not surprising considering the resolution of the coarse grid, where one grid cell has nearly the same spatial extent as the FIFE domain. Given this resolution

and the spatial variability of vegetation and soil characteristics, low correlations are expected. Although the bias for sensible heat fluxes is relatively small, the model does a poor job at simulating the temporal characteristics of sensible heat fluxes at this resolution. The bias for latent heat is relatively large considering that the magnitudes of latent heat flux for the period were generally tens of watts per square meter or less.

Examination of Table 2 for the short period, 1500–2100 UTC on the 11th, shows some improvement for the latent and sensible heat fluxes. The bias has decreased too, although the sign has changed for latent heat, indicating that the model underpredicts the magnitudes. The improvement is not surprising since the surface characteristics were specifically adjusted for this period. Table 3 indicates that the correlations are nearly perfect for temperature. The moisture field shows no improvement in terms of correlation; however, the bias has been reduced considerably.

The  $U$  component of velocity shows excellent agreement. Surprisingly the  $V$  component shows a negative correlation and a relatively strong negative bias of nearly  $1 m s^{-1}$ . The observations indicate that the wind shifted from northerly to southerly during the first 3 h of this period. The model predicts this wind shift to occur during the last hour of the period. It should be kept in mind that the model has already been integrated for 27 hours at the time of this analysis. Finally, the model was nudged at all points except the interior four

TABLE 3. Correlation coefficient, bias,  $E$ ,  $E_{UB}$ ,  $\sigma$ , and  $\sigma_{obs}$  for fine grid LES simulations computed from data covering 1515–2045 UTC.

Variable	$r$	Bias	$E$	$E_{UB}$	$\sigma$	$\sigma_{obs}$
$H$ ( $W m^{-2}$ )	0.20	-24	115	112	100	75
$\lambda E$ ( $W m^{-2}$ )	-0.07	19	62	59	43	38
$\lambda E$						
$(H + \lambda E)$	-0.027	0.06	0.21	0.20	0.13	0.11
$u$ ( $m s^{-1}$ )	0.66	0.46	0.98	0.86	1.0	1.1
$v$ ( $m s^{-1}$ )	-0.06	-0.90	1.3	0.98	0.77	0.56
$\theta$ (K)	0.97	0.04	0.79	0.79	2.9	2.4
$w$ ( $kg kg^{-1}$ )	0.03	0.0005	0.0007	0.0005	0.00008	0.0005

points of the coarse grid with the nudging strength 1/16 of that at the boundaries.

Also shown for the short period are some quantitative parameters calculated using the methodology of Keyser and Anthes (1977). The definition of  $E$ ,  $E_{\text{UB}}$ ,  $\sigma$ , and  $\sigma_{\text{obs}}$  is shown below, where  $\sigma_i$  and  $\sigma_{i_{\text{obs}}}$  are individual model results and observations at the same point, respectively;  $\sigma_o$  and  $\sigma_{o_{\text{obs}}}$  are the average values of  $\sigma_i$  and  $\sigma_{i_{\text{obs}}}$ , respectively; and  $N$  is the number of observations:

$$E = \left\{ \sum_{i=1}^{\#N} (\phi_i - \phi_{i_{\text{obs}}})^2 / \#N \right\}^{1/2}$$

$$E_{\text{UB}} = \left\{ \sum_{i=1}^{\#N} [(\phi_i - \phi_o) - (\phi_{i_{\text{obs}}} - \phi_{o_{\text{obs}}})]^2 / \#N \right\}^{1/2}$$

$$\sigma_{\text{obs}} = \left\{ \sum_{i=1}^{\#N} (\phi_{i_{\text{obs}}} - \phi_{o_{\text{obs}}})^2 / \#N \right\}^{1/2}$$

and

$$\sigma = \left\{ \sum_{i=1}^{\#N} (\phi_i - \phi_o)^2 / \#N \right\}^{1/2}.$$

Model skill is demonstrated when

$$\sigma \approx \sigma_{\text{obs}} \quad (1)$$

$$E_{\text{UB}} < \sigma_{\text{obs}} \quad (2)$$

and excellent skill when

$$E < \sigma_{\text{obs}}, \quad (3)$$

where  $E$  is the RMSE,  $E_{\text{UB}}$  the RMSE after a constant bias has been removed, and  $\sigma$  and  $\sigma_{\text{obs}}$  the standard deviations of the predictions and observations, respectively. Keyser and Anthes suggest that  $E_{\text{UB}}$  can show significant improvement over  $E$  since the constant bias is removed. They imply that the bias could be a result of an improper specification of the initial and/or bottom and lateral boundary conditions.

Table 2 shows that excellent skill is achieved for  $U$  and temperature. Latent heat, evaporative fraction, and mixing ratio also show skill according to the criterion. Only sensible heat fails to meet any of the criteria.

Point-by-point comparison of the model and the observations does provide a good demonstration of the model's ability to represent the momentum, temperature, and moisture fields, which were fairly homogeneous temporally and spatially. However, the applicability to fluxes is questionable. The FIFE domain is clearly subgrid in this case. A better measure of the models subgrid parameterization would be a correlation and bias applied to averaged values of the FIFE flux observations. When sensible and latent heat fluxes are averaged over all stations every 30 min for the 6-h time period, the resultant correlation jumps to 0.73 and 0.80 for sensible and latent heat fluxes, respectively. This indicates the RAMS subgrid parameterization is performing well.

Overall, the coarse grid simulation produces realistic representations of the fields over the vicinity of northeast Kansas and throughout the model domain. This is not surprising considering the model was nudged using analyzed fields and the case period modeled was under the influence of a broad high pressure system, which was relatively homogeneous.

### c. LES over FIFE for 11 October 1987

The previous section provides evidence of the coarse grid model's ability to simulate the large-scale flow over the region of northeastern Kansas, although finer structures are not resolved. The finer grids were integrated for 6-h starting at 1500 UTC 11 October 1987. The coarse mesh provided the large-scale forcing for the finer grids and it was hoped that the finest grid would provide details of conditions within the FIFE domain.

Following the methods used to analyze the coarse grid, correlations were computed for the observations and model fields at the same locations used to evaluate the coarse mesh employing the FIFE dataset during the 6-h period that the fine grids were integrated. Again, fields were averaged over 30-min intervals to facilitate direct comparison to the observations. The lowest level for the fine mesh was 200 m AGL, so similarity theory was used to ascertain the temperatures and winds at 2 m and 5.4 m AGL, respectively.

Shown in Table 3 are the computed correlations, bias,  $E$ ,  $E_{\text{UB}}$ ,  $\sigma$ , and  $\sigma_{\text{obs}}$  for the fine mesh. The same variables are evaluated as in the coarse mesh. The variability for all variables except  $w$  has increased, as evidenced by the increase in  $\sigma$ ; however, the skill in predicting has not been enhanced by the increased resolution. The correlations of  $U$  and  $V$  are less than for the coarse grid. As mentioned in the previous section, the wind shift was temporally displaced by about 4 hours. In addition, the coarse grid values of wind at the FIFE stations are a cubic spline interpolation from the four grid points around the FIFE domain. Thus, the interpolated values have information extracted from points where the wind shift has occurred, whereas the fine mesh will not contain this information. The biases for the wind components has also increased, again, probably due to the above reasoning.

The correlation for sensible heat and latent heat flux has degraded in this LES run. As mentioned previously, there were a few stations where downward latent heat fluxes were recorded, while the majority were directed upward. Although the fine grid added variability to the calculated fluxes, as demonstrated by an increase in magnitude of  $\sigma$ , the spatial locations where downward latent heat fluxes were calculated did not match the observed locations. At the same time, the coarse grid displayed little variability in latent flux. Thus, when the correlations were obtained from the fine grid there was a greater degree of variability and at the same time more error in the modeled fluxes. When an average flux for

TABLE 4. Comparison of  $H$  and  $\lambda E$  for observations, coarse grid, and fine grid at stations 1478, 2516, and 2043.

Time (UTC)	Station 1478						Station 2516						Station 2043					
	$H$ ( $W m^{-2}$ )			$\lambda E$ ( $W m^{-2}$ )			$H$ ( $W m^{-2}$ )			$\lambda E$ ( $W m^{-2}$ )			$H$ ( $W m^{-2}$ )			$\lambda E$ ( $W m^{-2}$ )		
	Obs	Coarse	Fine	Obs	Coarse	Fine	Obs	Coarse	Fine	Obs	Coarse	Fine	Obs	Coarse	Fine	Obs	Coarse	Fine
1645	387	259	234	-30	37	64	320	263	198	65	37	109	356	264	285	14	37	15
1715	398	304	259	-23	48	73	387	309	230	39	48	130	344	310	338	55	48	21
1745	396	337	293	-10	52	83	397	343	244	54	52	137	341	344	363	69	52	25
1815	394	358	304	-8	53	82	409	365	264	38	53	146	351	366	372	61	53	26
1845	332	370	323	49	52	84	397	378	265	45	52	145	334	378	388	67	52	27
1915	314	373	327	41	50	80	387	381	265	36	50	144	358	381	399	24	50	26
1945	296	365	314	36	46	71	368	372	263	33	46	141	293	373	381	61	46	23
2015	256	343	300	38	40	64	328	351	227	37	40	121	267	351	361	53	40	20
2045	209	306	260	34	33	52	283	313	208	45	33	110	229	314	319	48	33	16

all stations at each time is used and compared with the LES calculated fluxes, the correlations improve over a similar calculation performed on the coarse grid. For latent heat, a value of 0.80 is obtained for the correlation coefficient, with a bias of  $-25 W m^{-2}$ , while sensible heat has an  $r = 0.75$  and a bias of  $18 W m^{-2}$ . This could suggest that the flux calculations are not scale invariant contrary to the conclusion reached in Sellers et al. (1992).

An example of the model-calculated latent and sensible heat fluxes emphasizing this point is shown in Table 4. For station 2516, the fine grid largely overestimates latent heat during the period. The opposite can be said of station 2043. Station 1478 is an example of downward latent heat observed for part of the day. Neither coarse grid nor fine grid reproduce these observations. Finally, inspection of the coarse grid calculations clearly indicates a lack of variability as expected.

The results for the fine grid indicate a problem with the initialization of the finest mesh. Since the large-scale fields of  $U$ ,  $V$ , temperature, and mixing ratio were reproduced fairly well, it was determined that there was some bias in the initialization of the soil moisture, which has a direct impact on the heat fluxes calculated by the model. Another source of error could be in the vegetation parameters determined from the observations. This was dismissed since the LAI and canopy heights determined from observations had adequate spatial coverage and a relative lack of sensitivity to these parameters, when compared to soil moisture, as determined from previous simulations.

#### d. Development of a soil initialization technique

In the previous section we saw that the model did actually predict downward latent heat fluxes, although they were spatially inaccurate. Examination of latent heat fluxes for the entire model domain indicated a spread similar to the observations in terms of maximum and minimum sensible and latent fluxes. This suggests that it might be possible to calibrate soil moisture if there is a direct relation between the latent heat and the soil moisture in the model data. A study by Cuenca et

al. (1996) suggests the need to calibrate the soil properties on a case basis instead of using the Clapp and Hornberger formulation directly. Chen and Brutsaert (1995) develop a linear formula for relating soil moisture in the top 0.10 m to the latent heat flux. They also include such parameters as LAI and green vegetation fraction (GVF) in successive formulas with little improvement over using soil moisture only.

Figure 2 shows a scatterplot of initial model soil moisture, averaged through a 0.075-m depth and 6-h averaged latent heat flux for the entire model domain at points where short grass (Fig. 2a) and tall grass (Fig. 2b) were present. The figure demonstrates that a linear relationship could be used for determining the soil moisture based on the observed average latent heat fluxes. Deviations from a linear fit are likely due to different vegetation characteristics such as LAI, fractional coverage, roughness length, and transpiration rates. Figure 2 shows that the relationship for soil moisture and latent heat flux diverge somewhat as the soil moisture passes roughly 40% of capacity. The two classes dominant in the FIFE domain are tall and short grass (over 98% of the vegetation coverage was one of the two). Other classes were filtered out of the analysis.

The data from the scatterplot was used to determine a best-fit line, using a least squares linear regression technique. The slope and intercept values were then used in conjunction with the station observations (20 stations in all) of 6-h averaged latent heat fluxes to determine an initial soil moisture at the given site. The top soil layer was given twice the weight as the 0.025-m level, which in turn was weighted twice as much as the next level, 0.075 m. The slope intercepts in equations are nearly identical. Chen and Brutsaert determined an intercept of 0.173. The slope parameter is different since their value multiplied the ratio of observed latent heat to the equilibrium evaporation rate, whereas the equation derived here uses the observed latent heat average. Their relationship was also derived over five different IFCs.

The derived soil moistures were then used in the objective analysis to determine the new soil moisture fields. The soil moisture for the surface, 0.025-m, and

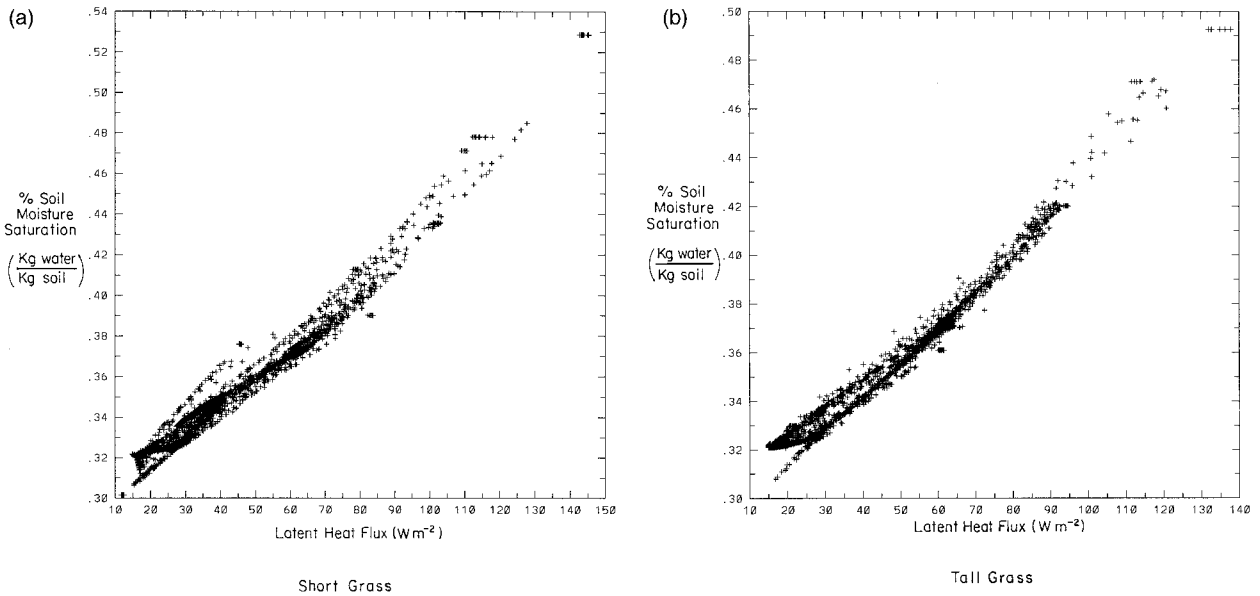


FIG. 2. Scatterplot of initial model soil moisture and 6-h-averaged latent heat flux for the entire model domain for (a) short grass and (b) tall grass.

0.075-m levels was determined from the weights in the regression equation. The ratio of the new soil moisture at 0.075 m and the old value at that level was then used to adjust soil levels below 0.075 m.

*e. Analysis of the adjusted soil moisture LES simulation*

The simulation using the soil moisture adjustments prescribed in the above formulation were started from the same initial conditions as the other simulation. All variables except moisture were kept constant between the simulations. Following the analysis of the previous simulations, Table 5 shows the correlation, bias,  $E$ ,  $E_{UB}$ ,  $\sigma$ , and  $\sigma_{obs}$  for the runs with recalibrated soil moisture.

It is clear there has been significant improvement. Of particular interest are the variables for the surface energy budget. The correlation for both latent and sensible heat has improved: roughly doubled for sensible and six times larger in the case of latent heat. Also note the bias has switched sign for both latent and sensible heat, with

the bias for latent heat reduced by roughly two-thirds. In the case of latent heat, the RMSE is now less than  $\sigma_{obs}$ , indicating the ability of the model to simulate latent heat. Although the RMSE with and without the bias is still larger than  $\sigma_{obs}$  for sensible heat, it has been reduced and is approaching  $\sigma_{obs}$ . In conjunction with the improvement in model skill for latent and sensible heat, the evaporative fraction has changed from basically no skill to a high correlation and meets the standard of the most stringent test on the relation of RMSE and  $\sigma_{obs}$  for latent heat and evaporative fraction.

Table 6 shows the station data and modeled results for the three stations displayed in Table 4. Station 1478, which shows a change from negative latent heat to positive values over the 6-h period, indicates the model agrees with the observations initially. However, the change in sign is not predicted, with values nearing zero by the end of the simulation. Station 2043, which showed the model underpredicting latent heat, is now well represented, implying the soil adjustment was successful. The prediction at the other station, 2516, has

TABLE 5. Correlation coefficient, bias,  $E$ ,  $E_{UB}$ ,  $\sigma$ , and  $\sigma_{obs}$  for the fine grid after soil moisture reinitialization using data from 1515 through 2045 UTC.

Variable	$r$	Bias	$E$	$E_{UB}$	$\sigma$	$\sigma_{obs}$
$H$ ( $W m^{-2}$ )	0.47	-8.5	93	93	100	75
$\lambda E$ ( $W m^{-2}$ )	0.50	3.5	35	34	30	38
$\frac{\lambda E}{(H + \lambda E)}$	0.54	0.007	0.10	0.10	0.10	0.11
$u$ ( $m s^{-1}$ )	0.66	0.35	0.96	0.89	1.1	1.1
$v$ ( $m s^{-1}$ )	-0.04	-1.2	1.5	0.95	0.74	0.56
$\theta$ (K)	0.94	0.67	1.1	1.2	3.2	2.4
$w$ ( $kg kg^{-1}$ )	-0.30	0.0004	0.0007	0.0005	0.00009	0.0005



TABLE 6. Comparison of  $H$  and  $\lambda E$  for observations and fine grid at stations 1478, 2516, and 2043.

Time (UTC)	Station 1478				Station 2516				Station 2043			
	$H$ ( $\text{W m}^{-2}$ )		$\lambda E$ ( $\text{W m}^{-2}$ )		$H$ ( $\text{W m}^{-2}$ )		$\lambda E$ ( $\text{W m}^{-2}$ )		$H$ ( $\text{W m}^{-2}$ )		$\lambda E$ ( $\text{W m}^{-2}$ )	
	Obs	Model	Obs	Model	Obs	Model	Obs	Model	Obs	Model	Obs	Model
1645	387	311	-30	-18	320	277	65	26	356	254	14	58
1715	398	348	-23	-17	387	315	39	32	344	301	55	68
1745	396	382	-10	-16	397	343	54	36	341	310	69	69
1815	394	401	-8	-13	409	357	38	38	351	350	61	72
1845	331	418	49	-11	397	367	45	39	334	353	67	67
1915	314	402	41	-8	387	364	36	39	358	360	24	63
1945	296	398	36	-6	368	353	33	37	293	350	61	56
2015	256	367	38	-5	328	340	37	34	267	322	53	46
2045	209	322	34	-5	283	294	45	28	229	299	48	39

also improved. Previously it was overpredicted by a factor of about 3. The station-by-station results were improved at all stations analyzed, as demonstrated by these results and the correlations and skill scores for the flux quantities. This suggests that the technique was applicable over the range of soil moistures. The domain-averaged fluxes, when model and observations were correlated, showed no change in terms of the correlation coefficient; however, the bias was less than half the previous values for sensible heat, and was reduced by a factor of 6 for latent heat.

## 5. Summary and conclusions

A simulation of a golden day, 11 October 1987, of FIFE was performed with an LES embedded within coarser grids. This day was chosen since winds were light, allowing mesoscale circulations to provide important contributions to the predicted flow fields. The day was atypical of golden days in that winds are relatively weaker than the other golden days of FIFE 1987 and 1989.

An evaluation of the coarse grid was undertaken to ascertain the skill of the RAMS in simulating 11 October 1987. The model validation was completed using NCAR archived surface observations and two temporal subsets of the FIFE87 dataset. It was shown that the coarse mesh reproduced the dynamic and thermodynamic fields observed. When a point-by-point comparison of latent and sensible heat flux and evaporative fraction was performed using the FIFE flux station data, the model did not perform well at coarse resolutions. However, when spatially averaged quantities of the fluxes were compared to the spatially averaged model quantities, a significant increase in correlation coefficients was achieved, demonstrating skill in the turbulent closure scheme implemented in the RAMS model.

An LES run was then conducted for a 6-h period on 11 October 1987. It was found that again the model did reproduce the spatially averaged flux measurements for this period. The results indicated that added variability of computed quantities was enhanced and that the spread of these quantities was similar to those observed. The

spatially averaged prediction of the model heat fluxes also correlated with the observations. Errors in the spatial patterns of the heat fluxes were determined to be significantly controlled by the values of the surface soil moisture. A method was then used to invert the observed temporally averaged latent fluxes into an initial soil moisture to be used by the model.

The LES were then integrated again using the adjusted soil moisture. It was found that the model's ability to predict sensible and latent heat flux, as well as evaporative fraction, increased. Point-by-point comparison between flux station data and the model showed increased skill for all flux quantities, with little change in wind, moisture, and temperature fields.

This study points out a need for calibration of the surface moisture. This result is unique in that it was applied to a fully 3D LES of the FIFE domain versus point models where it is generally applied. Overall, the results demonstrate the model's skill in reproducing the highly variable surface energy budget for 11 October 1987 within the FIFE domain. This implies that the model should reproduce boundary layer characteristics and secondary circulations that have been observationally documented for the FIFE domain.

*Acknowledgments.* This work was supported in part by the the National Aeronautics and Space Administration under Grant NAG5-2078, United States Geological Survey, Department of the Interior under Assistance 1434-94-A-1275, and the National Science Foundation under Grant ATM-9306754.

## REFERENCES

- Avisar, R., and Y. Mahrer, 1988: Mapping frost-sensitive areas with a three-dimensional numerical model. Part I: Physical and numerical aspects. *J. Appl. Meteor.*, **27**, 400–413.
- , and R. A. Pielke, 1989: A parameterization of heterogeneous land surfaces for atmospheric numerical models and its impact on regional meteorology. *Mon. Wea. Rev.*, **117**, 2113–2136.
- Charpentier, M. A., and P. M. Groffman, 1992: Soil moisture variability within remote sensing pixels. *J. Geophys. Res.*, **97**, 18 987–18 995.
- Chen, C., and W. R. Cotton, 1983: A one-dimensional simulation of

- the stratocumulus-capped mixed layer. *Bound.-Layer Meteor.*, **25**, 289–321.
- , and —, 1987: The physics of the marine stratocumulus-capped mixed layer. *J. Atmos. Sci.*, **44**, 2951–2977.
- Chen, D., and W. Brutsaert, 1995: Diagnostics of land surface spatial variability and water vapor flux. *J. Geophys. Res.*, **100**, 25 595–25 606.
- Clapp, R. B., and G. M. Hornberger, 1978: Empirical equations for some soil hydraulic properties. *Water Resour. Res.*, **14**, 601–604.
- Cuenca, R. H., M. Ek, and L. Mahrt, 1996: Impact of soil water property parameterization on atmospheric boundary-layer simulation. *J. Geophys. Res.*, **101**, 7269–7277.
- Dalu, G. A., R. A. Pielke, M. Baldi, and X. Zeng 1996: Heat and momentum fluxes induced by thermal inhomogeneities. *J. Atmos. Sci.*, **53**, 3286–3302.
- Dickinson, R. E., A. Henderson-Sellers, P. J. Kennedy, and M. F. Wilson, 1986: Biosphere atmosphere transfer scheme for the NCAR community climate model. Tech. Rep. NCAR/TN-275+STR, NCAR, 69 pp. [Available from NCAR, P.O. Box 3000, Boulder, CO 80307.]
- Gal-Chen, T., and R. C. J. Somerville, 1975: On the use of a coordinate transformation for the solution of the Navier–Stokes equations. *J. Comput. Phys.*, **17**, 209–228.
- Keyser, D., and R. A. Anthes, 1977: The applicability of a mixed-layer model of the planetary boundary layer to real-data forecasting. *Mon. Wea. Rev.*, **105**, 1351–1371.
- Klemp, J. B., and R. B. Wilhelmson, 1978a: The simulation of three-dimensional convective storm dynamics. *J. Atmos. Sci.*, **35**, 1070–1096.
- , and —, 1978b: Simulations of right- and left-moving storms produced through storm splitting. *J. Atmos. Sci.*, **35**, 1097–1110.
- Mahrer, Y., and R. A. Pielke, 1977: A numerical study of the airflow over irregular terrain. *Beitr. Phys. Atmos.*, **50**, 98–113.
- McCumber, M. C., and R. A. Pielke, 1981: Simulation of the effects of surface fluxes of heat and moisture in a mesoscale numerical model. Part I: Soil layer. *J. Geophys. Res.*, **86**(C10), 9929–9938.
- Nicholls, M. E., R. A. Pielke, J. L. Eastman, C. A. Finley, W. A. Lyons, C. J. Treback, R. L. Walko, and W. R. Cotton, 1995: Applications of the RAMS numerical model to dispersion over urban areas. *Wind Climate in Cities*, J. E. Cermak et al., Eds., Kluwer Academic, 703–732.
- Peck, E. L., and A. S. Hope, 1995: Spatial patterns of soil moisture for the FIFE study area derived from remotely sensed and ground data. *J. Geophys. Res.*, **100**, 25 463–25 468.
- , T. R. Carroll, and D. M. Lipinski, 1992: Airborne soil moisture measurements for First International Satellite Land Surface Climatology Program Field Experiment. *J. Geophys. Res.*, **97**, 18 961–18 967.
- Pielke, R. A., J. S. Baron, T. G. F. Kittel, T. J. Lee, T. N. Chase, and J. M. Cram, 1992: Influence of landscape structure on the hydrologic cycle and regional and global climate. *Proc. Managing Water Resources During Global Change*, Reno, NV, Amer. Water-Resour. Assoc., 283–296.
- Sellers, P. J., F. G. Hall, G. Asrar, D. E. Strebel, and R. E. Murphy, 1992: An overview of the First ISLSCP Field Experiment. *J. Geophys. Res.*, **97**, 18 455–18 466.
- Shuttleworth, W. J., and J. S. Wallace, 1985: Evaporation from sparse crops—An energy combination theory. *Quart. J. Roy. Meteor. Soc.*, **111**, 839–855.
- Treback, C. J., and R. Kessler, 1985: A surface temperature and moisture parameterization for use in mesoscale numerical models. Preprints, *Seventh Conf. on Numerical Weather Prediction*, Montreal, PQ, Canada, Amer. Meteor. Soc., 355–358.
- Tripoli, G. J., and W. R. Cotton, 1982: The Colorado State University three-dimensional cloud/mesoscale model—1982. Part I: General theoretical framework and sensitivity experiments. *J. Rech. Atmos.*, **16**, 185–220.
- Ungar, S. G., R. Layman, J. E. Campbell, J. Walsh, and H. J. McKim, 1992: Determination of soil moisture distribution from impedance and gravimetric measurements. *J. Geophys. Res.*, **97**, 18 969–18 977.
- Vidale, P. L., R. A. Pielke, A. Barr, and L. T. Steyaert, 1997: Mesoscale circulations and their effects over the BOREAS domain. *J. Geophys. Res.*, in press.
- Wai, M. M.-K., and E. A. Smith, 1998: Linking boundary-layer circulations and surface processes during FIFE 89. Part II: Maintenance of secondary circulation. *J. Atmos. Sci.*, **55**, 1260–1276.
- Wang, J. R., S. P. Gogineni, and J. Ampe, 1992: Active and passive microwave measurements of soil moisture in FIFE. *J. Geophys. Res.*, **97**, 18 979–18 985.